Case Studies in Construction Materials 20 (2024) e02721

Contents lists available at ScienceDirect

Case Studies in Construction Materials

journal homepage: www.elsevier.com/locate/cscm

Interfacial adhesion between recycled aggregate and asphalt mastic filled with recycled concrete powder

Bin Lei [a], Wanying Yang [a], Yipu Guo [b,*], Xiaonan Wang [b], Qianghui Xiong [a], Kejin Wang [c], Wengui Li [d,*]

[a] School of Infrastructure Engineering, Nanchang University, Jiangxi 330031, China
[b] School of Civil and Environmental Engineering, University of Technology Sydney, NSW 2007, Australia
[c] Department of Civil, Construction and Environment Engineering, Iowa State University, IA 50011, USA
[d] Centre for Infrastructure Engineering and Safety, School of Civil and Environmental Engineering, The University of New South Wales, NSW 2052, Australia

ARTICLE INFO

Keywords:
Recycled concrete powder
Recycled aggregate
Interfacial adhesion
Asphalt mastic
Binder bond strength test
Surface free energy method

ABSTRACT

Recycled aggregate (RA) and recycled concrete powder (RCP) hold significant potential as environmentally sustainable raw materials for asphalt mixtures. In this study, a comprehensive investigation was conducted on the bonding properties between RA and RCP-filled asphalt mastic (RCPAM). This investigation utilized an image processing-assisted modified water boiling test, binder bond strength (BBS) tests, and the surface free energy (SFE) method. The results indicate that the boiling water test method, even with the assistance of 2D image processing analysis, cannot adequately evaluate the adhesive characteristics of the RA-RCPAM interface. This limitation could be attributed to the relatively small number of samples tested and the significant variation in surface properties of RA. Increasing both the filler-to-asphalt (F/A) ratio and RCP replacement ratio adversely affected the interfacial bond strength of the RA-RCPAM interface. On the other hand, an increase in RA surface roughness contributed to a higher bond strength. Based on the experimental results, a best-fit multivariate mixed model was proposed to predict the interfacial bond strength between RCP-filled asphalt mastic and recycled aggregate within a given range of RCP replacement ratio, surface roughness, and filler-to-asphalt (F/A) ratios. The analysis of SFE suggested that moisture damage to RCPAM was caused by both cohesive and adhesive failure. Additionally, the minimal impact of adhesion work in wet condition with increasing RCP content suggested that adhesion failure energy was only marginally affected by the inclusion of RCP, even in the presence of moisture. These findings are expected to enhance the understanding of interfacial adhesion characteristics and moisture susceptibility of the RA-RCPAM interface.

1. Introduction

The structural stability, durability and service life longevity of asphalt pavement are closely correlated to the bond properties between asphalt and aggregate under different conditions [1–3]. The interfacial bonding strength is generally dependent on the physiochemical properties of both aggregate and asphalt. The adhesion of asphalt to aggregate will be negatively impacted once the

* Corresponding authors.
E-mail addresses: yipu.guo-1@student.uts.edu.au (Y. Guo), wengui.li@unsw.edu.au (W. Li).

https://doi.org/10.1016/j.cscm.2023.e02721
Received 4 October 2023; Accepted 24 November 2023
Available online 28 November 2023

water infiltrates the asphalt pavements and erodes the aggregate-asphalt interface, subsequently inducing the moisture damage [4,5]. Moisture damage can degrade the overall performance of the interlocking structures in asphalt concrete and further induce other visible road distresses and diseases, such as stripping, ravelling, mesh cracks, potholes, etc. [6]. In many countries such as China and the United States, the deterioration of asphalt pavements and associated maintenance costs are primarily attributed to moisture damage of asphalt [2,4]. Consequently, enhancing the interfacial adhesion between asphalt and aggregate is the key to prevent water damage.

On the other hand, as the shortage of natural resources such as natural sand and stone become increasingly serious, the feasibility of using recycled coarse aggregate (RA) and recycled concrete powder (RCP) sourced from construction and demolition (C&D) waste in asphalt mixture has received increasing attention [7–9]. RCP is a powder with the particle size less than 0.075 mm resulting from the process of manufacturing RA of demolished concrete, and it accounts for approximately 15–20 % of the total mass of construction solid waste [10,11]. Recently, there are increasing studies regarding the application of RCP as cement replacement or additives in cement-based composites [12–14]. RCP contains a large amount of hardened cement products and unhydrated cement clinkers, which is associated with the characteristics of high porosity and rough surface [12,15]. It has been preliminarily shown that it is feasible to replace mineral powder with RCP as asphalt mixture filler to modify asphalt [16,17]. The concept of composite use of RCA to replace natural aggregate and RCP to replace mineral powder filler in concrete or asphalt mixture can maximum the recycling rate of C&D waste to efficiently confront the urgent issues brought by C&D waste disposal. Therefore, the composite use of RA and RCP recycled from concrete into asphalt pavement is a promising approach to the development of sustainable construction.

There are three types of interface in asphalt concrete made with RCA: the interface between RA and asphalt is comprised by the interface 1: new asphalt is adhered to the mortar of RCA, interface 2: new asphalt is direct adhered to old natural aggregate, and interface 3: the interface between old mortar and natural aggregate as shown in Fig. 1. In general, the influential factors affecting the interfacial adhesion performance of asphalt-aggregate system can be categories into the asphalt properties (i.e., chemical composition, contact angle and wax content), aggregate properties (e.g., alkali value and surface structure) and external environmental factors such as temperature, and moisture [18,19]. Owing to the presence of highly developed flaws and pores inside the cement mortar of RCA, moisture can easily intrude into the interfacial phase of aggregate-asphalt system and subsequently lead to a more severe deterioration of interfacial adhesion for RA compared to natural aggregates [20]. In addition, since adhesion is mainly stemmed from the microscopic forces between the contacting interfaces which involves both physical and chemical interactions that are highly dependent on the surface micromorphology and chemical composition of the materials [21,22], the microscopic mechanism of interfacial adhesion between RA and asphalt is further complicated [23].

Gomez-Meijide et al. [24] found that the adhesion between RA and asphalt was similar to the counterpart between natural aggregate and asphalt by adopting the boiling method, while the rolling bottle method showed that the adhesion between RA and asphalt was found to be much more inferior to the counterpart between natural aggregate and asphalt. According to Huang et al. [20], the adhesion interface of old mortar and asphalt of RA was more irregular and convex in comparison to the natural limestone aggregate. In addition, the adhered cement mortar was found to have looser structures, which was considered as the worst in the RA components by correlating nanomechanical properties in the interfacial transition zone with the adhesion of RA-asphalt interface. Wang et al. [25] correlated the surface morphology characteristics of four types of coarse aggregate to the quantitative results of adhesion evaluations methods of surface energy method and shear strength test. There was a good positive correlation between multiscale surface morphologies and adhesive bonding between the aggregates and cement emulsified asphalt. Pasandin and Perez [26] pointed out that the surface of recycled aggregate generally had rough surface texture and rich angularity, asphalt binder was prone to fills up the micro superficial pores and voids and intrude into the aggregate, leading to compact asphalt-stone structure, as well as the enhanced interfacial adhesion and water stability of asphalt-aggregate system. Based on the boiling test, Lei et al. [27] attained the adhesion grade of the RA-asphalt interface of four, which was increased to five by modifying RA by the pretreatment methods of slurry encapsulation, silicone resin solution immersion and calcium hydroxide solution immersion. Similarly, the adhesion grade of RA-asphalt interface upgraded from four to five after the activation of organic silicone resin [23]. Zhang et al. [28] proposed that the degraded interfacial adhesion between RA and asphalt was ascribed to the reaction between water-soluble ions leaching from the old mortar adhered in recycled aggregate and carboxylic acid components in asphalt.

Although some efforts have been made, the investigations on the interfacial adhesion between RA and asphalt are still limited and the findings are somehow contradictory and show the large variability, which is probably ascribed to the fact the highly inhomogeneity of RA induces the of different and complex phase compositions, aggregate sizes, surface structures, and surface chemistry [24,29]. The mechanisms behind macroscale adhesive behaviors of RA-asphalt interface require further explorations from multiscale perspectives. More significantly, there is lack of investigation on the adhesion between RA-asphalt interface in the asphalt mixture containing RA and RCP, which is ideal for developing green and sustainable pavements. Nevertheless, RA is often considered to present reasonably

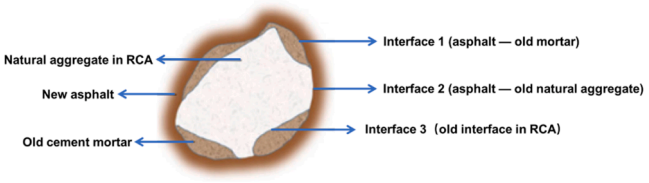

Fig. 1. Interface morphology of recycled aggregate and asphalt.

high quality than RCP because RCP contains multiple impurity components that are hard to remove [30]. The adhesion between aggregate and asphalt may be impacted with the inclusion of RCP and the interaction between RCP and asphalt is still unclear [31,32]. In addition, our previous study confirmed that the F/A ratio has the significant effect on specific properties of RCP filled asphalt mastic [33]. Along these lines, multiple experimental and theoretical evaluation methods including image processing-assisted modified water boiling test, binder bond strength (BBS) test and surface free energy (SFE) method were used to comprehensively evaluate the interfacial adhesion properties between RA and RCPAM prepared with various F/A ratio and RCP replacement ratio and explore the mechanisms behind adhesion formation and failure [34–37].

2. Experimental program

2.1. Materials and preparation

2.1.1. Raw materials

The granite-typed RA used in this study was derived from the abandoned concrete blocks dismantled from domestic buildings (Nanchang, China). The 13.2–16.0 mm RA particles were used to prepare the specimens. RCP is sourced from broken C40 concrete samples. RCP with the particle smaller than 0.075 mm was obtained by further crushing, grinding, and sieving. The other RA is the modelled recycled aggregate (MRA), which is described in Section 2.1.3. The commercially available limestone powder (LSP) has an apparent density of 3036 kg/m^3 with only 0.2 % moisture content. RCP was dried for 48 h in an oven at 60 ℃ to reach a constant weight. Type P.O. 42.5 Ordinary Portland cement conforming to Chinese standard GB175–2007 was adopted to prepare the modelled recycled aggregate [38]. Table 1 lists physical properties of RCP and LSP, which are in accordance with the requirements of JTG F40–2017 [39]. Table 2 lists the chemical compositions of RCP and LSP. Table 3 lists physical properties of RA. The morphologies of raw materials are shown in Fig. 2.

2.1.2. Preparation of RCP filled asphalt mortar

Three filler to binder (F/A) ratios (0.6, 0.9, and 1.2) as per recommended by JTG F40–2017 [39] and five RCP replacement ratios (0, 25 %, 50 %, 75 %, and 100 %) for the replacement of LSP were designed in this study. The mix proportions of the asphalt mastics are illustrated in Table 4. The preparation of asphalt mastic and its properties are detailed in Ref. [33].

2.1.3. Preparation of modelled recycled aggregate

To investigate the effect of RA surface roughness on the adhesion properties of the RA-RCPAM interface, it is necessary to prepare the RA with various roughness while simplifying the other influential and heterogeneous factors such as coating rate of adhered old mortar or irregular aggregate shape. For this purpose, four kinds of MRA specimens with the different roughness of 0 mm, 0.05 mm, 0.10 mm, and 0.15 mm were innovatively designed and manufactured in this study, with the consideration of that the actual RA is difficult to characterize the surface roughness and meet such requirement. Roughness refers to the average depth per unit surface area [40]. The modelled recycled aggregate is prepared by means of pouring the fresh cement paste with a water-to-cement ratio of 0.4 to the pre-designed MRA molds. The molds for manufacturing MRA specimens are composed of five Acrylonitrile-butadiene-styrene (ABS) plastic plates including one bottom plate and four side plates, which are assembled with adhesive tape tightly. As shown in Fig. 3, the different roughness of MRA specimens is realized by the raised circle with a diameter of 20 mm in the middle of the mold bottom plate. Fig. 3(a) indicates that the bottom plate is a circle with a middle bulge of 1 mm and a diameter of 20 mm, corresponding to the roughness is 0 mm. As shown in Fig. 3(b), (c), and (d), ribs of various heights of 1 mm, 2 mm, and 3 mm were uniformly distributed on the bulge with the constant width and gap of 2 mm, corresponding to the roughness of 0.05 mm, 0.1 mm, and 0.15 mm, respectively. The MRA molds and MRA specimens with four degrees of roughness are shown in Fig. 3(e) and (f), respectively.

2.2. Experimental methods

2.2.1. Image processing-assisted modified boiling test

The adhesion property of RCP filled asphalt was evaluated by boiling water test according to JTGE20–2011 (T 0616–1993) [41], which covers several steps displayed in Fig. 4: 1) Five recycled aggregate particles with size distribution of 13.2–19 mm were washed and dried in 105 ± 5 ℃ oven until the mass of the specimens reaching mass equilibrium; 2) These particles were immersed in the pre-heated asphalt mastic (130–150 ℃) for 45 s; 3) The asphalt coated particles were hung up at 25 °C to naturally cool for 15 min; 4) These particles were boiled in water for 3 min; and 5) Based on the percentage of peeling area, the test results were visually classified

Table 1
Physical properties of LSP and RCP.

Type of fillers	Apparent density (g·cm^{-3})	Hydrophilic coefficient	Moisture content (%)	Content of particle size <0.075 mm (%)
LSP	3.036	0.72	0.2	93.56
RCP	2.684	0.81	0.3	94.21
Requirements in JTG F40–2017 [39]	≥2.500	<1.00	<0.5	≥85.0

Table 2
Chemical compositions of RCP and LSP.

Filler	CaO	SiO_2	Al_2O_3	Fe_2O_3	K_2O	MgO	Na_2O	SO_3	LOI
LSP (%)	92.1	1.5	0.8	4.1	—	0.8	—	—	0.7
RCP (%)	50.0	27.3	10.2	2.3	2.0	4.5	0.7	1.1	2.2

Table 3
Physical properties of RA.

Apparent density	Water absorption	Crushing index	Size distribution
2531 kg/m^3	4.0 %	17.6 %	13.2–16.0 mm

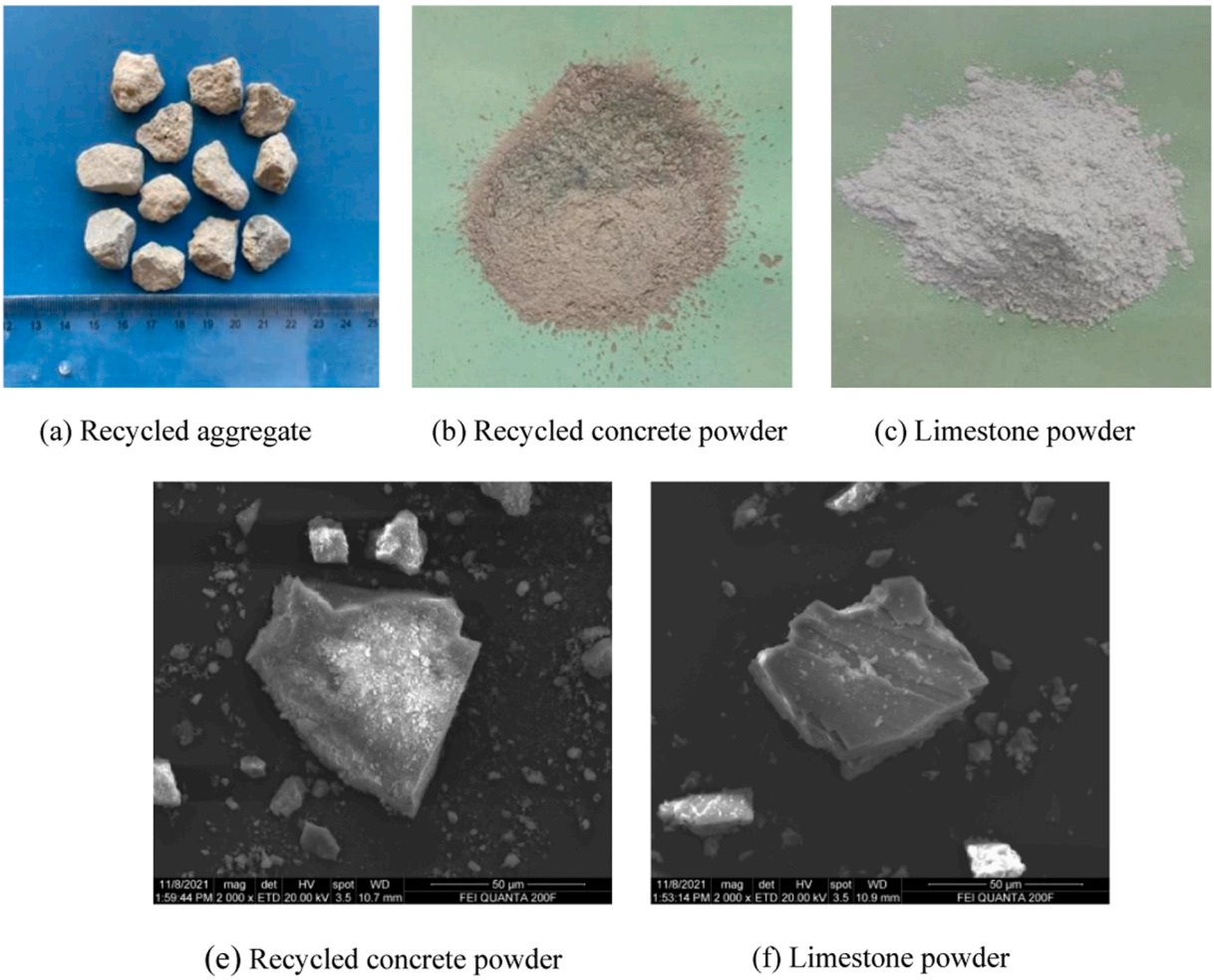

Fig. 2. Macro and micro morphologies of raw mineral materials.

into five grades from 1 to 5 defined in JTGE20–2011 (T 0616–1993) to illustrate various peeling conditions and adhesion grades of asphalt binder on the surface of RA. The grade '1′ indicates that the asphalt film is thoroughly moved by water whereas the grade '2′ indicates that the asphalt film is completely preserved. Five replicates for individual groups to perform the parallel tests.

In order to avoid the above evaluation defects of boiling method, the image processing method is further applied on specimens. As illustrated in Fig. 5, the pixel of aggregate entire surface (P_1) and pixel of asphalt binder peeling area (P_2) were processed and captured by Photoshop software. The peeling rate of asphalt binder on recycled aggregate can be calculated by Eq. (1). It is worthy mentioned that although certain discrepancy exists between the 2D photo recognition surface and the actual 3D surface, 2D image analysis enables a primary quantitative assessment.

Table 4
Mix proportion of RCP filled asphalt mastics.

Specimens	Filler to binder (F/A) ratio	Recycled concrete powder (RCP) replacement ratio (%)	Limestone powder (LSP) content (%)
RCPAM-0.6–0 %	0.6	0	100
RCPAM-0.9–0 %	0.9	0	100
RCPAM-1.2–0 %	1.2	0	100
RCPAM-0.6–25 %	0.6	25	75
RCPAM-0.6–50 %	0.6	50	50
RCPAM-0.6–75 %	0.6	75	25
RCPAM-0.6–100 %	0.6	100	0
RCPAM-0.9–25 %	0.9	25	75
RCPAM-0.9–50 %	0.9	50	50
RCPAM-0.9–75 %	0.9	75	25
RCPAM-0.9–100 %	0.9	100	0
RCPAM-1.2–25 %	1.2	25	75
RCPAM-1.2–50 %	1.2	50	50
RCPAM-1.2–75 %	1.2	75	25
RCPAM-1.2–100 %	1.2	100	0

Notes: RCPAM denotes the RCP filled asphalt mastic. (e.g., RCPAM-0.6–75 % represents the RCP filled asphalt mortar with the F/A ratio of 0.6 and the RCP replacement ratio of 75 %)

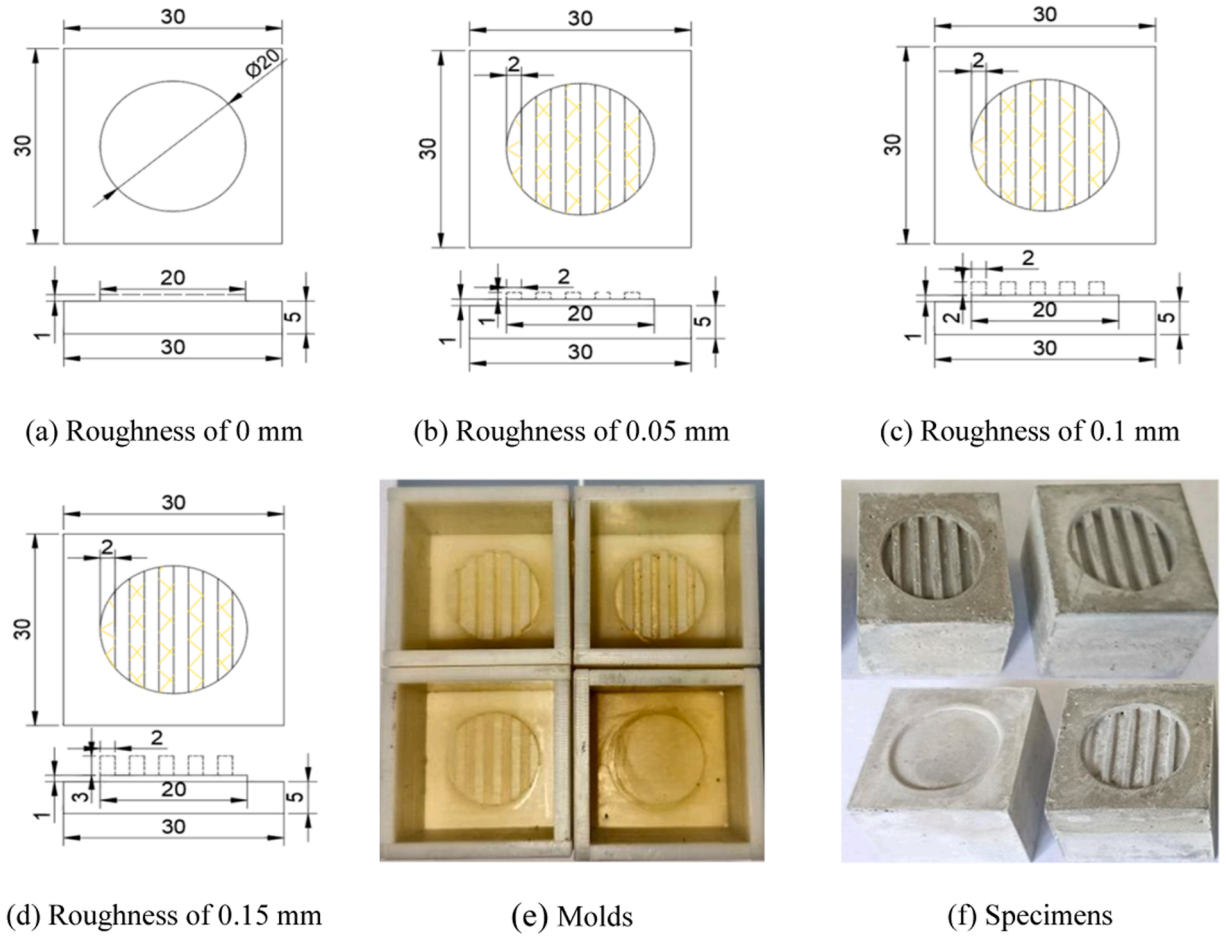

Fig. 3. Schematical diagram of bottom plates of modelled recycled aggregate molds and prepared specimens with different surface roughness (size in mm).

$$\text{Peeling rate} = \frac{P_2}{P_1} \times 100\% \quad (1)$$

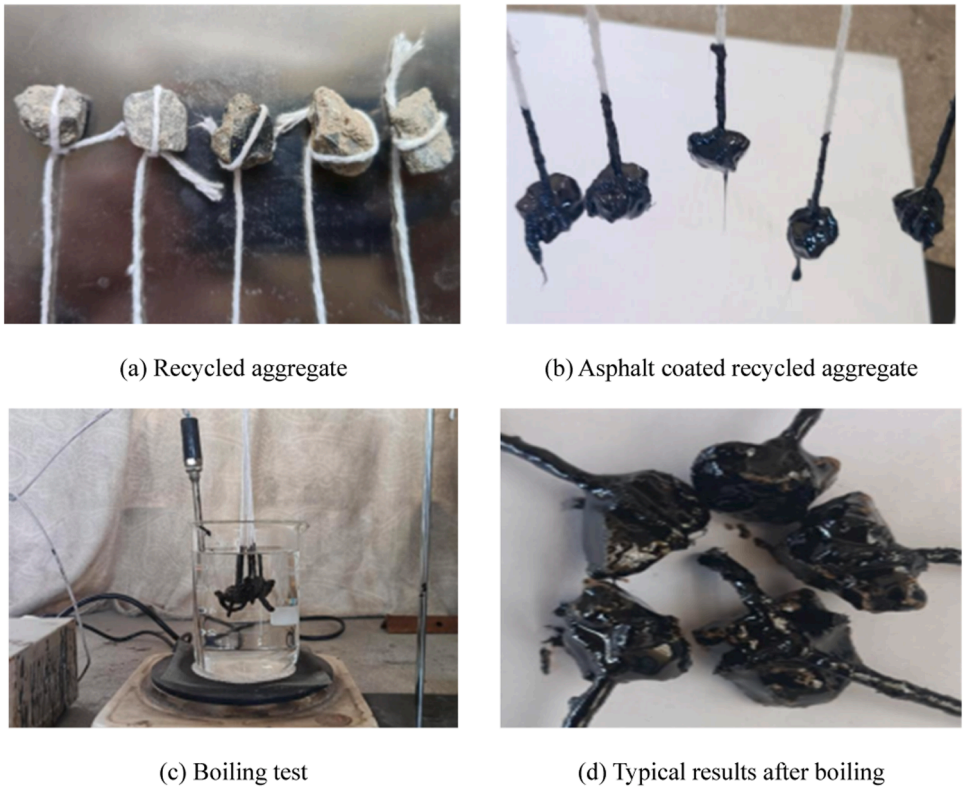

Fig. 4. Boiling water test process for recycled aggregates.

2.2.2. Binder bond strength (BBS) test

The Binder Bond Strength (BBS) test in accordance with the standard test method (ASTM D 4541) has been widely reported in studies to assess the bonding strength between asphalt–aggregate interface [42,43]. The BBS test was conducted by a Posi Test At-A apparatus (De Felsko, USA). In this study, the adhesion properties of RCPAM to MRA with different surface roughness were studied through modified BBS testing. To prepare the testing samples, the modelled aggregate substrate and BBS pull-stubs were heated at 135 ℃ for drying. The melted asphalt mastic samples were withdrawn into the pre-designed groove on the MRA surface and held in oven for further 30 min to enable the asphalt naturally to flow smooth in Fig. 6(a). In order to evaluate the moisture susceptivity of actual asphalt-aggregate system, the pull-stubs sealed samples were immersed in 50 ℃ water bath for 24 hr, as shown Fig. 6(b). Prior to the BBS test, the tested samples were conditioned in water bath at 5 ℃ for 2 hr and pull-out tensile strength (POTS) was tested using Posi Test At-A apparatus. The testing loading rate was 0.7 MPa/s. 3 parallel tests were conducted for each group to assure the accurate analysis. Samples without water bath treatment were also tested for comparation.

2.2.3. Surface free energy (SFE) method

The SFE method is employed to investigate the cohesion and adhesion energies of LCPMA and RCPMA based on the tested contact angle. There are two essential steps to prepare the asphalt samples with a smooth and flat surface in Fig. 7(a), the dryness plain-glass slides (25 × 75 mm) were immersed into melted asphalt mastic and withdrawn immediately after that the asphalt mastic fully wraps two-thirds of the slides, then being held for a while until the excessive asphalt mastic drops. Subsequently, put the asphalt coated glass slide in a 135 ± 5 ℃ oven for 30 mins. The contact angle of naturally cool downed RCPMA and MRA samples are tested by a drop shape analyzer (Dataphysics OCA20, Germany). Two reagents, distilled water and diiodomethane, were employed as the standard liquids to determine the cohesion and adhesion works based on the SFE theory. The selected reagent (3–5 μL) was dropped into tested samples through a needle in Fig. 7(d). According to SFE theory, the amounts of cohesion and adhesion works can be calculated based on Eqs. (2) to (5).

$$r_{regent}(1+\cos\theta) = 2\sqrt{r^{d}_{asphalt} \bullet r^{d}_{reagent}} + 2\sqrt{r^{p}_{asphalt} \bullet r^{p}_{reagent}} \tag{2}$$

The cohesion work for RCPMA can be determined as :

$$W_c = 2r_{asphalt} \tag{3}$$

The adhesion work in dry condition can be determined as:

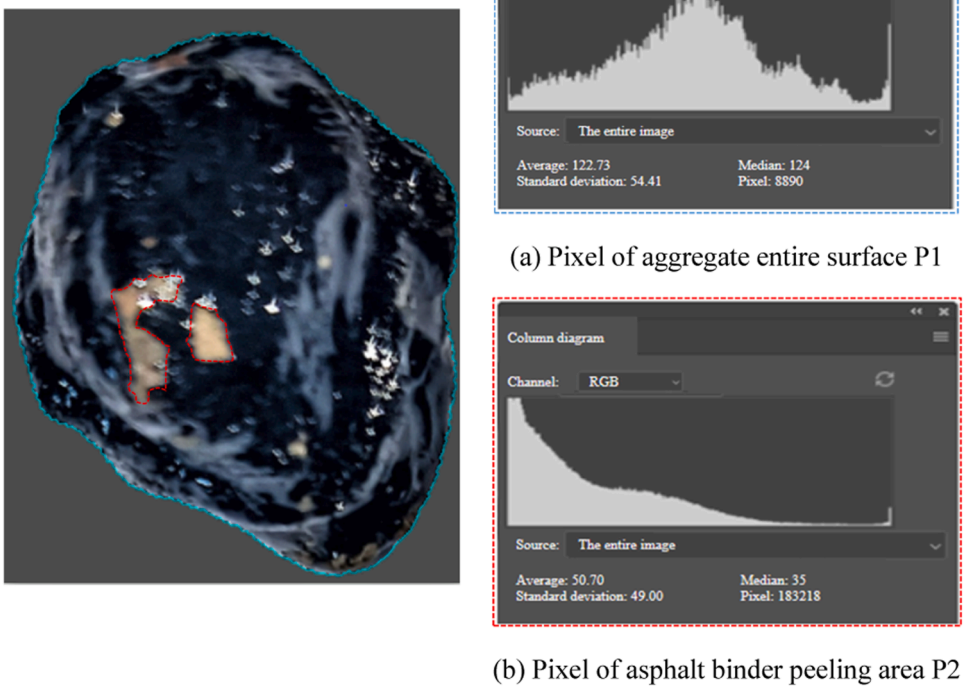

Fig. 5. Image processing method for aggregates.

$$W^{a}_{dry} = 2(\sqrt{r^{d}_{asphalt} \bullet r^{d}_{aggregate}} + 2\sqrt{r^{p}_{asphalt} \bullet r^{p}_{aggregate}} \tag{4}$$

The adhesion work in wet condition can be determined as:

$$W^{a}_{wet} = 2(r_{water} + \sqrt{r^{d}_{asphalt} \bullet r^{d}_{aggregate}} + 2\sqrt{r^{p}_{asphalt} \bullet r^{p}_{aggregate}} - \sqrt{r^{d}_{asphalt} \bullet r^{d}_{water}} - \sqrt{r^{p}_{asphalt} \bullet r^{p}_{water}} - \sqrt{r^{d}_{aggregate} \bullet r^{d}_{water}} - \sqrt{r^{p}_{aggregate0} \bullet r^{p}_{water}}) \tag{5}$$

where θ denotes the contact angle of asphalt with regents; $r^{superscript}_{subscript}$ is the surface free energy; Superscripts d and p represent the dispersive (Lifshitz-van der Waals) component of surface energy and polar (Lewis acid-base) component of surface energy, respectively; Subscript represents the asphalt, reagent, aggregate and water.

3. Results and discussions

3.1. Image processing-assisted modified boiling test

3.1.1. Boiling water test results

The boiling water test is regarded as qualitative method for evaluating the moisture susceptibility potential of asphalt [44]. Fig. 8 displays the results of boiling water test. According to JTG E20–2011, the majority of groups are graded as '5′, which signifies that the asphalt mastic film is thoroughly retained, and the peeling area is almost 0. As shown in Fig. 8(d), (m) and (0), only the groups RCPAM-1.2–0 %, RCPAM-1.2–25 %, and RCPAM-1.2–75 % with recycled aggregate are graded as '4′, meaning that asphalt film is locally retained on the surface of the aggregate and the percentage of peeled area is greater than 30 %. The spalling area of asphalt mastic is the surface area of natural aggregate, whereas there is almost no asphalt spalling in the old cement mortar area. The natural aggregate part in spalling areas is granite that is classified as acidic rock, in which the SiO_2 content is greater than 63 % generally possesses poor binding to asphalt [5]. The boiling test results indicate that the inclusion of RCP seems not to degrade the adhesion between asphalt and RA. Moreover, it seems that the larger F/A slightly reduces the grade of adhesion between asphalt and RA.

3.1.2. Image processing analysis

To mitigate the disadvantage that visual inspection is not such precise, the image processing is employed to obtain more

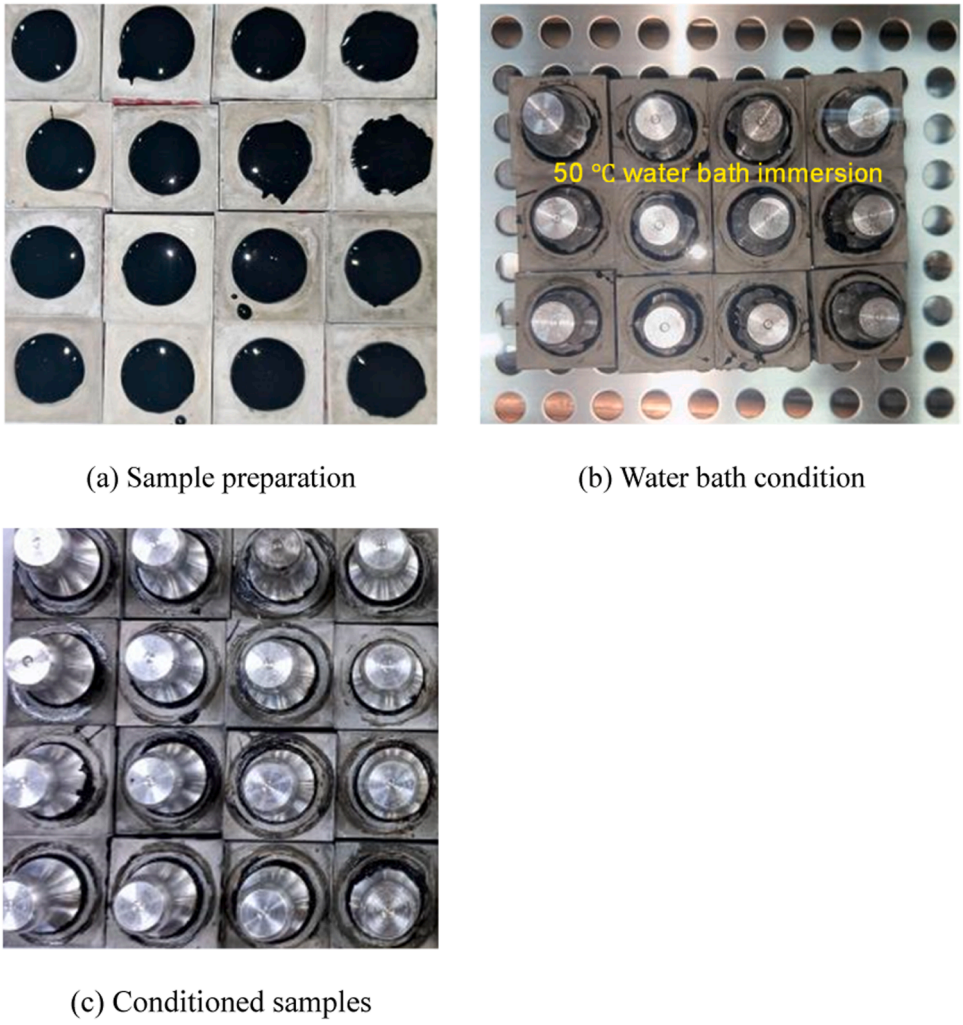

Fig. 6. Preparation of binder bond strength test samples.

quantitative results. Fig. 9 presents the peeling rate of all groups of asphalt mastic calculated based on Eq. (1). It is seen that the peeling rate of asphalt mastic on the surface of recycled aggregate for the majority groups is all below 5 % except for the groups of RCPAM-1.2–25 % and RCPAM-1.2–75 %. In addition, the peeling rate increases with the increase of the F/A. The peeling rates of RCPAM-0.6–0 %, RCPAM-0.9–0 %, and RCPAM-1.2–0 % are increased by 0.16 %, 1.72 %, and 2.76 %, respectively compared with the base asphalt, which is consistent with the test results in literature [45]. Because with the increase of the filler content, light components such as aromatic and saturated components in asphalt are absorbed and their content decreases, thereby leading to the degradation of adhesive property of asphalt mastic [46]. The peeling rate value for RCPAM-25 % seems to be an outlier value. Overall, the imaging processing method shows the consistent results with the visual observation. Nevertheless, the variation trend of peeling rate shows no obvious regularity with the increase of RCP replacement ratio, which is inconsistent with the results obtained from the SFE and BBS methods by which the effect of RCP content can be properly characterized by these two quantitative methods. Although the image processing method is adopted to assist the boiling test in this study and the results are averaged from five parallel test to acquire the quantitative results, it is unsuitable to evaluate the adhesive characteristics between RA and RCPAM. This is contrary to some previous studies that evidenced that image processing method could accurately and effectively measure the asphalt peeling ratio and thus provide the accurate evaluation of moisture susceptibility and adhesive characteristics of asphalt-aggregate systems [1,2,47,48]. This is probably attributed to the fact that in comparison to the natural aggregate including limestone, granite, gravel and basalt [47–49] or steel slag [47] tested in previous studies, the surface of recycled concrete has the more complex nature due to existence of attached old mortar and rich angularity, which is substantiated by large variability in the results of parallel specimens. Moreover, the volume of natural aggregate in each of the RA particles may significantly vary, which can lead to large variation of the test results. For some specimens, it seems that the asphalt was not peeled form the old mortar portion in RA but from the natural aggregate, such as those in Fig. 8(a). Additionally, the sample size adopted in the present study which is only five parallel specimens for one group may be insufficient to capture the variation regularity.

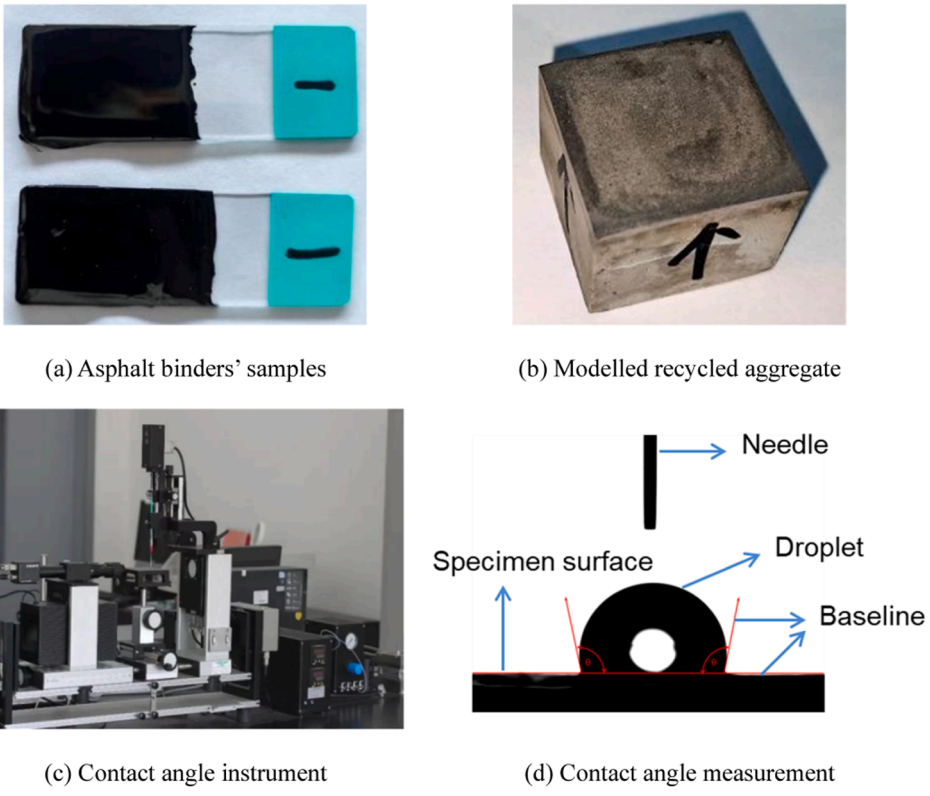

Fig. 7. Sessile drop test process.

3.2. BBS method

3.2.1. BBS results

There are two types of bond failure in asphalt-aggregate system: cohesive failure and adhesive failure. Cohesive failure occurs when the cohesive strength of asphalt is smaller than the adhesive strength between asphalt and aggregate substrate [50], whereas adhesive failure occurs in the case that cohesive strength of asphalt is larger than the adhesive strength between asphalt and aggregate substrate [44]. The BBS test is performed on asphalt – MRA substrate system. The failure type for all specimens in normal temperature are always found to be cohesive in Fig. 10 (a). This phenomenon is consistent with the SFE results as discussed later that W_c^a is always less than W_{dry}^a, which confirms that the cohesive failure is the most common failure form for RCPAM specimens without external water and water erosion is unfavorable for the bond strength. Moreover, in consistent with the SFE result that W_{dry}^a is lower than W_{wet}^a, which reveals that the adhesive failure between RCPAM and MRA is mainly caused by the water damage. All specimens under wet condition (i.e., subject to 50 ℃ water bath treatment) show the adhesive failure in Fig. 10 (b). The POTS values obtained from the adhesive failure type can be used to evaluate the adhesion properties of asphalt-aggregate system.

Fig. 11 (a) to (d) illustrate POTS values from wet condition ($POTS_{wet}$) of 70-base asphalt and RCPAM to MRA with increasing roughness from 0 to 0.15 mm. It can be seen with the increasing of surface roughness, the averaged $POTS_{wet}$ value increases by 18.1 %, 36.9 %, and 55.0 %, respectively for F/A ratios of 0.6, 0.9 and 1.2. The interfacial adhesion between asphalt and aggregate is mainly ascribed to the micro-nano physical and chemical actions on the surfaces [50,51]. Pumping and infiltration are considered as the main forms of asphalt binder injecting into the aggregate surface, which forms a crisscross interface [52]. Under the action of mechanical occlusion and chemical adsorption, two materials contact at interface and bond together. With the increase of surface roughness of the aggregate, the effective contact area and mechanical interlocking strength accordingly increase, leading to the increase of $POTS_{wet}$ value [21]. The effect of surface roughness of aggregate seems to be opposite with the counterpart of asphalt binder, which is mainly ascribed to the fact that the surface roughness of the aggregate is on the micrometer scale whereas the counterpart of asphalt binder is on the nanoscale [53].

In terms the effects of RCP replacement ratio and F/A ratio, it is seen that the $POTS_{wet}$ shows a declined trend with the increase of both ratios. When comparing RCPAM-100 % with RCPAM-0 %, the maximum drop of 24.36 % happens when F/A ratio is 0.6 and surface roughness is 0.05. In addition, as illustrated in Fig. 12, the F/A ratio of 0.9 batch and surface roughness of 0.1 batch show the most obvious drop trend than other batches when solely making the comparison in terms of F/A ratio and surface roughness. The results obtained from the from BBS test seems to be inconsistent with the counterparts from SFE method (surface roughness of 0 mm batch). The most obvious declining trend in $POTS_{wet}$ happens at F/A ratio of 0.9 and the most obvious trend in adhesion work in wet

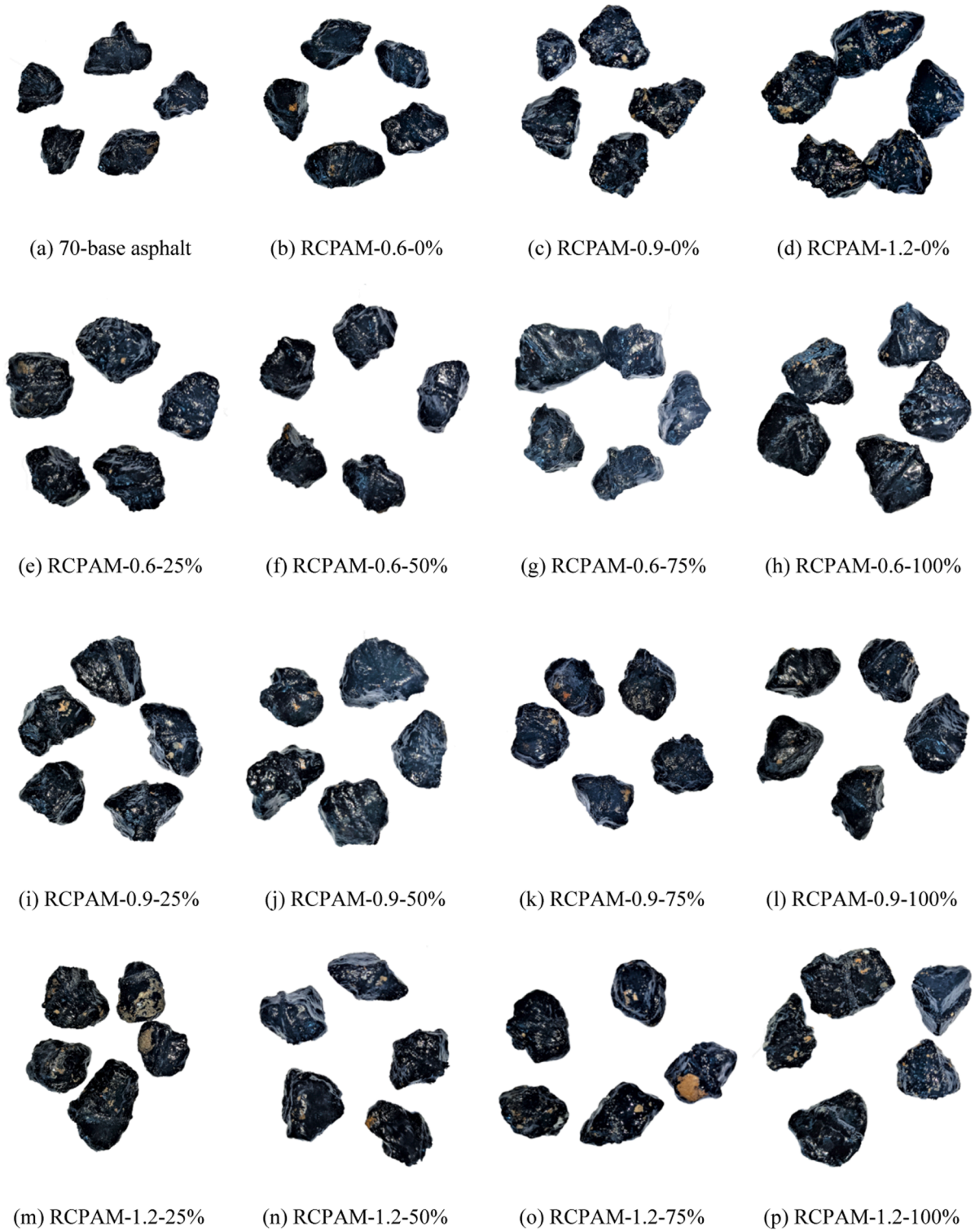

Fig. 8. Boiling water test results of recycled aggregates.

condition (W^{a}_{wet}) happens at F/A of 1.2, which reveals the potential inconsistent results brought by theoretical analysis method (SFE) and actual experimental method (BBS). Some contradictory results between BBS and SFE methods are also obtained in previous studies [44,54], hence it should be caution when single evaluation method for moisture resistance of asphalt mixtures is used alone [55]. Since

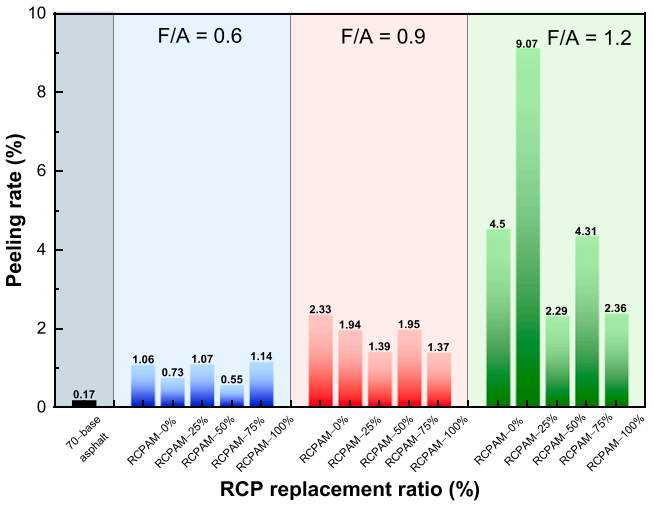

Fig. 9. Peeling rate of RCP filled asphalt mastic on recycled aggregate.

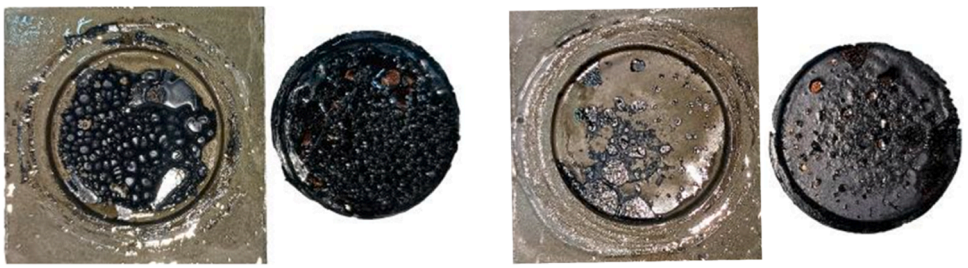

(a) Cohesive failure (failure in asphalt matrix)

(b) Adhesive failure (failure at the asphalt – MRA aggregate interface)

Fig. 10. Cohesive failure and adhesion failure in BBS test.

there is no adhesion between filler and aggregate, the increase of F/A ratio will comprise the effective content and contact area between asphalt binder and aggregate, thereby reducing the binding force between asphalt binder and aggregate [33].

3.2.2. *Multivariate regression analysis*

Previous analysis indicates that RCP replacement ratio, surface roughness and F/A ratio apparently influence adhesion properties of asphalt binder-aggregate system. To further explore the inherent relationships between these influential factors and bond strength of asphalt binder–aggregate system, multiple regression analysis method that can establish linear or nonlinear mathematical correlations between multiple variables is carried out by adopting single variable as a response dependent variable (RDV) and other variables as independent variables (IVs). The conventional multivariate regression model can be expressed as follows:

$$\text{Linear model1}, Y = \beta_1 \bullet X_1 + \beta_2 \bullet X_2 + \cdots + \beta_k \bullet X_k + \alpha \tag{6}$$

where α and β are regression constants. Y denotes the RDV of $POTS_{wet}$; and X_k is the IV pertaining to the RCP replacement ratio, surface roughness and F/A ratio (k = 3). The values of IVs are 0, 25, 50, 75, 100 (RCP replacement ratio, %), 0, 0.05, 0.10, 0.15 (Surface roughness, mm), 0.6, 0.9, 1.2 (F/A ratio). In addition, previous studies [56–58] adopted the following nonlinear and mixed multivariate models that were expressed in multivariate linear formats to achieve more accurate regression results, by taking the natural logarithm of aforementioned conventional linear function or incorporating the mixed IVs.

$$\text{Nonlinear model2}, \mathrm{Ln}(Y) = \beta_1 \bullet X_1 + \beta_2 \bullet X_2 + \cdots + \beta_k \bullet X_k + \alpha \tag{7}$$

$$\text{Nonlinear model3}, \mathrm{Ln}(Y) = \beta_1 \bullet \mathrm{Ln}(X_1) + \beta_2 \bullet \mathrm{Ln}(X_2) + \cdots + \beta_k \bullet \mathrm{Ln}(X_k) + \alpha \tag{8}$$

$$\text{Mixed model from4to}(k+3), X_k \Big/ Y = \sum_{j=1}^{k} \beta_j \bullet X_j + \alpha \ , \ j = 1, \ldots, k \tag{9}$$

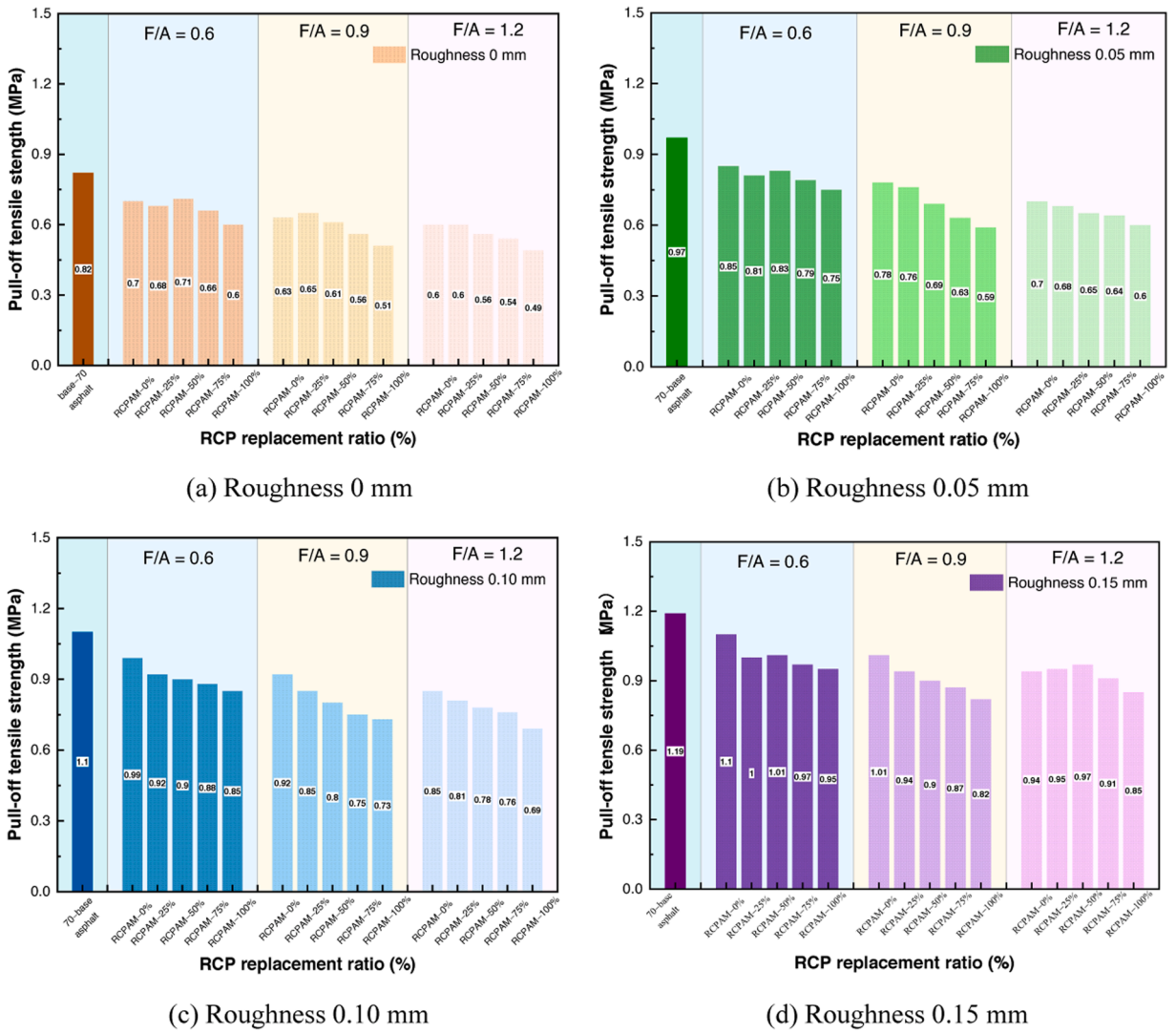

Fig. 11. $POTS_{wet}$ values of base-asphalt and RCPAM to MRA with different surface roughness.

$$\text{Mixed model from}(k+4)\text{to}(2k+3), \mathrm{Ln}(X_k \Big/ Y) = \sum_{j=1}^{k} \beta_j \bullet \ln(X_j) + \alpha \ , \ j = 1, \ldots, k \tag{10}$$

As listed in Eqs. (6), (7), (8), (9), and (10), a total of 9 multivariate regression model (1 linear, 2 nonlinear and 5 mixed models) were analyzed for the RSV of $POTS_{wet}$. Generally, the increased number of sample data is beneficial for the multivariate regression results [56]. A total number of 60 sample data were performed for multivariate regression analysis with the assistance of SPSS software. Variance and residual analysis were carried out for each model and the significance of individual influential factor was tested. The regression results of RDV of $POTS_{wet}$ relative to the IVs of RCP replacement ratio, surface roughness, and F/A ratio were detailed in Table 5. D-W value can be utilized to diagnose the autocorrelation of model residual deviations. The optimal D-W value is in the range of 1.5–2.5 and is preferably close to 2.0.

As indicated in Table 5, most models present the good degree of fitting substantiated by R^2 value greater than 0.9. The mixed model 6 presents the largest R^2 of 0.976. With the comprehensive consideration of R^2 and D-W value, the best-fit multivariate model in predicting the $POTS_{wet}$ is identified as:

$$\mathrm{Ln}X_R/POTS_{wet} = 1.014 + 0.35\mathrm{Ln}(X_R) - 0.35\mathrm{Ln}(X_S) + 2.354\mathrm{Ln}(X_F) \tag{11}$$

The R^2 and D-W values of the best-fit model are 0.960 and 1.919, respectively. The histogram and cumulative probability of standard residuals of the best-fit model are illustrated in Fig. 13. As shown in Fig. 13 (a), the distribution of standardized residuals generally complied with the normal distribution, with the highest frequency is presented at zero residual value. In addition, as displayed in Fig. 13 (b), all residual values are generally uniformly distributed in two sides of the 45-degree diagonal of the cumulative

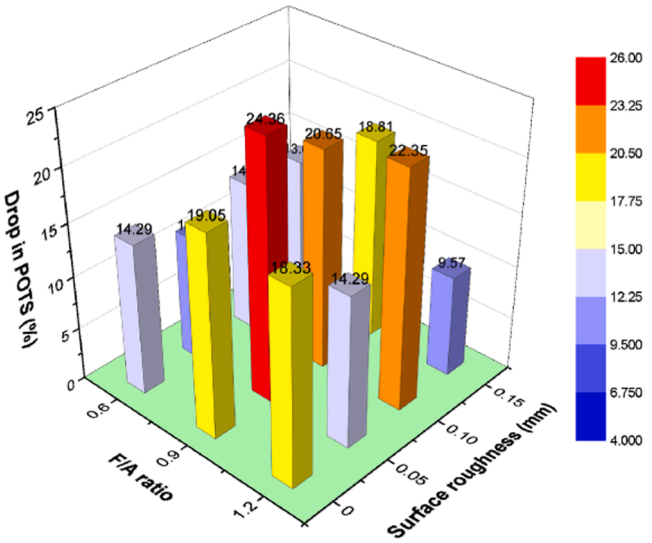

Fig. 12. Percentage drop in $POTS_{wet}$ from RCPAM-0 % to RCPAM-100 % with different F/A ratio and surface roughness.

Table 5
Regression results of adhesion behavior for MRA-RCPAM interface.

Regression models (Model No.)											
Linear model				Nonlinear models				Mixed models			
No.	RDV	R^2	D-W value	No.	RDV	R^2	D-W value	No.	RDV	R^2	D-W value
1	$POTS_{wet}$	0.957	0.870	2	$\ln(POTS_{wet})$	0.951	0.795	4	$X_L/POTS_{wet}$	0.976	1.503
				3	$\ln(POTS_{wet})$	0.775	0.556	5	$Xs/POTS_{wet}$	0.974	0.631
								6	$X_F/POTS_{wet}$	0.952	0.546
								7	$\ln(X_R)/POTS_{wet}$	0.960	1.919
								8	$\ln(X_S)/POTS_{wet}$	0.909	0.610
								9	$\ln(X_F)/POTS_{wet}$	0.812	0.522

Note: R^2 refers to the goodness of fit; D-W value refers to Durbin-Watson statistical results; X_L, X_C and X_A are the abbreviations of IVs of the LCP replacement ratio, surface roughness and F/A ratio. Since value of 0 cannot be proceeded with the natural logarithm, all 0 values in sample data are replaced by 0.001 to perform the regression analysis.

probability distribution graph (Theoretical normal hypothesis VS sample observations), further evidencing the reliability of the normal distribution hypothesis of sample residuals.

Table 6 lists the representative results of analysis of variance (ANOVA) and the effects of individual factor (RCP replacement ratio, surface roughness and F/A ratio) based on model 1 (linear regression), for the purpose of assessing the overall significance of the model

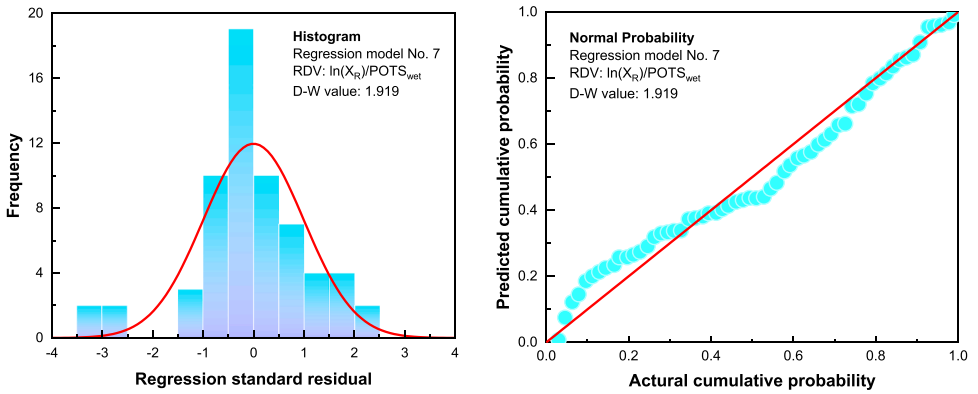

(a) Standardized residual histogram (b) Normal probability

Fig. 13. Standardized residual histogram and normal probability for the best-fit regression model.

and influential degree of various IVs. It is seen that F value of model 1 is distinctively higher than $F_{0.01}$ of 4.459 and $F_{0.05}$ of 2.901, suggesting that there is overall significant multivariate regression relationship between $POTS_{wet}$ and various influential IVs. Manifested by the P values less than 0.05, the results of T-test that evaluates the impact of individual influential IV on target RDV indicate that surface roughness possesses a significantly positive influence whereas RCP replacement ratio and F/A ratio possess a significantly negative influence on the bond strength of RA-RCPAM interface under wet condition ($POTS_{wet}$). In addition, the higher T value pertaining to surface roughness implies that surface roughness poses a more significant impact on $POTS_{wet}$ in comparison to RCP replacement ratio and F/A ratio, while the comparable T values pertaining to RCP replacement ratio and F/A ratio demonstrate their similar influential degree on $POTS_{wet}$.

3.3. SFE method

Fig. 14 lists the result of contact angle measurements. Fig. 15 illustrates the variations in surface energy of melted RCPAM with different F/A ratio calculated from contact angle measurements. There is no consistent trend for polar component with increasing RCP replacement ratio among asphalt mastic with different F/A ratio. When F/A ratio is 0.6, the polar component is increased with increase of RCP replacement ratio, while opposite trend is found when F/A ratio increases to 1.2. Compared to polar component, dispersive component of surface energy occupies the much higher proportion than polar component. The surface energy of 70-base asphalt and MRA are 35.1 and 54.4, respectively. The surface energy of RCPAM-0.6–0 %, RCPAM-0.9–0 %, RCPAM-1.2–0 % are decreased by 2.9 %, 6.6 %, and 14.5 % compared with the base asphalt, respectively. This is caused by the fact that LSP possesses the low-polar characteristic, and can be interacted with the asphalt to vary the surface structure of the asphalt [59]

Fig. 16 (a) and (b) compares variations in dispersive component of surface energy of and cohesion work of asphalt mastic. The cohesion work refers to the reversible work to separate an object per unit area into two sections and form two new interfaces [60,61]. Fig. 17 (a) shows variations in adhesion work of RCPAM and MRA under dry conditions. The adhesion work refers to the reversible work to separate a two-phase interface per unit area into two sections and form two new interfaces. The higher the adhesion work, the more stable and stronger interface and better adhesion between two-phase materials [61]. It is seen that overall variation trends between dispersive component of surface energy, adhesion work between recycled aggregate and asphalt are similar, evidencing the dominating role of dispersive component in cohesion property within RCPAM and adhesion property of RA-RCPAM interface. It is seen that dispersive component of surface energy ($\gamma_{asphalt}$), cohesion work (W_c), and adhesion work in dry condition (W^a_{dry}) unfavorably decrease with the increase of F/A ratio and RCP replacement ratio. Evidenced by increased steepness of slope of the fitting curves shown in Fig. 16 and Fig. 17 (a), RCP content has limited effect on the $\gamma_{asphalt}$, W_c, and W^a_{dry} of RCPAM when F/A are 0.6 and 0.9, whereas RCP content shows more significant effect F/A is 1.2. The W^a_{dry} of RCPAM-0.6–100 %, RCPAM-0.9–100 %, RCPAM-1.2–100 % are decreased by 4.75 %, 6.22 % and 12.1 %, respectively.

To further evaluate the moisture susceptibility of the RCPAM, the adhesion work between RA and RCPAM in wet condition (W^a_{wet}) is shown in Fig. 17 (b). It is seen that variations of W^a_{wet} show no obvious trend in terms of F/A ratio and RCP replacement ratio. The values for all group are very limitedly fluctuated at approximately 25.5 ± 1 mJ/m^2. Different from W_c and W^a_{dry}, the inclusion of RCP does not pose any jeopardizing affect the W^a_{wet}. The presented results suggest that the inclusion of RCP is detrimental to the cohesion and adhesion under dry condition while has no obvious influence for adhesion of RA-RCPAM system under wet condition.

Previous studies agree that the adhesion work between asphalt and recycled aggregate in wet condition has a close relationship with the aggregate sizes, surface structures, and surface chemistry [23,24]. The complex source of recycled aggregate and bitumen further complicate their chemical properties [24,29]. Recycled aggregate has the complex chemical compositions as mortar contains a certain amount of cement hydration products such as C-S-H, $Ca(OH)_2$ monosulfide-type sulphoaluminate, and ettringite. These products weak chemical reactions with acidic asphalt [23]. Since the dispersive component mainly reflects the non-polar part of the van der Waals force, which is closely associated with the surface structure characteristics of the tested samples [62], the inclusion of RCP affects the surface chemistry and surface structure, thereby causing the unfavorably negative impact to both cohesion and adhesion in dry condition. Overall, the degradations of both cohesion and adhesion under dry condition with increasing RCP content imply that the moisture damage of RCPAM is stemmed from its both cohesive and adhesive failure [44]. While the imperceptible impact of W^a_{wet} with increasing RCP content suggests that adhesion failure energy is limitedly impacted by the inclusion of RCP with the presence of moisture. Accordingly, the water stability of RCPAM pavement may not be inferior to the LCP filled pavement in actual environment.

3.4. Correlation between BBS and SFE methods

Fig. 18 illustrates the correlations between $POTS_{wet}$ in terms of W_c, W^a_{dry} and W^a_{wet}. As shown in Fig. 18 (a) and (b), the cohesion work and adhesion work in dry condition possess the good positive correlation with $POTS_{wet}$, with the correlation factors above 0.69. Higher W_c and W^a_{dry} are associated with a higher bond strength for RA-RCPAM interface. Since a higher cohesion of asphalt mastic requires a higher energy to cause the pull-off failure and asphalt mastic with a higher W^a_{dry} is harder to strip from the aggregate, it is indicated pull-off failure of RCPAM-RA system in wet BBS test is stemmed from both the cohesive failure of asphalt and adhesive failure of asphalt-aggregate interface [44]. Different from W_c and W^a_{dry}, W^a_{wet} is insignificantly correlated with the bond strength of RCPAM-RA system, which is substantiated by the unsatisfactory correlation factors shown in Fig. 18 (c). This reveals that there is not significant correlation between W^a_{wet} and bond strength for RCPAM-RA system, which shows a good agreement with the fact that the adhesion

Table 6
ANOVA and individual influencing factor results based on Model 1.

Model (IVs)	F Value	T Value	P Value
ANOVA	421.027	—	—
RCP replacement ratio	—	-11.459	0.000
Surface roughness	—	31.035	0.000
F/A ratio	—	-11.899	0.000

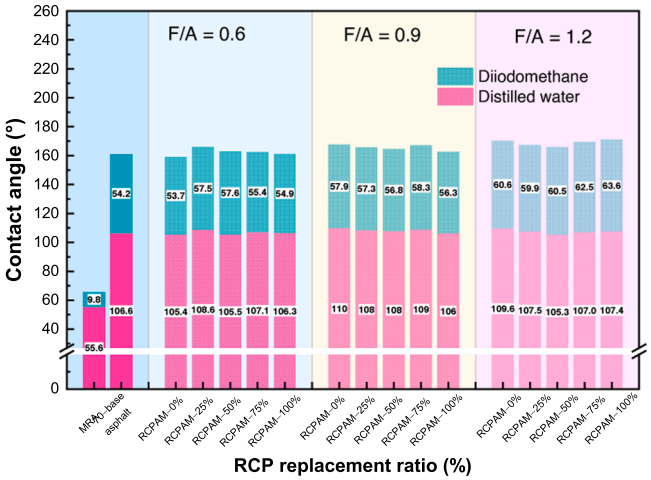

Fig. 14. Contact angle between asphalt mastic and test liquid.

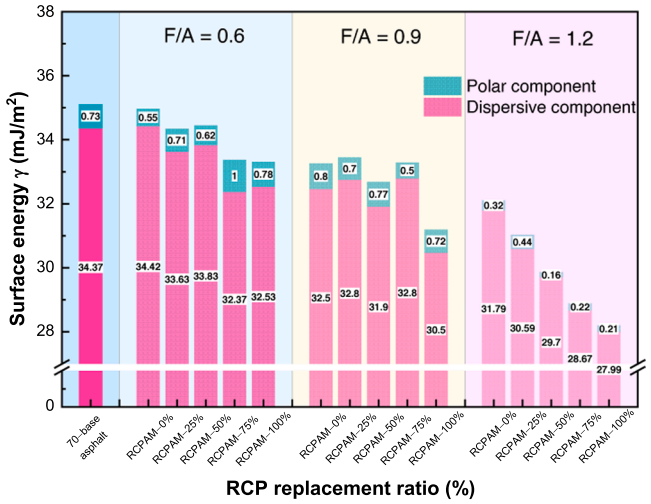

Fig. 15. Variations of surface energy in terms of RCP replacement ratio for RCPAM with different F/A ratio.

failure energy of RCPAM-RA system is limitedly impacted by inclusion of RCP with the presence of moisture.

4. Conclusions

This study investigated the adhesion and moisture susceptibility of the RA-RCPAM interface. Three methods were employed, including image processing-assisted modified water boiling test on recycled aggregate, binder bond strength (BBS) test, and surface free energy (SFE) method on modelled recycled aggregate. The results obtained from these methods are compared and analyzed. Specifically, the influence of the surface roughness of RA on the interfacial adhesion characteristics between RA and RCPAM was examined using the innovatively prepared MRA in the BBS test. Based on the experimental and theoretical findings, the following conclusions can be drawn:

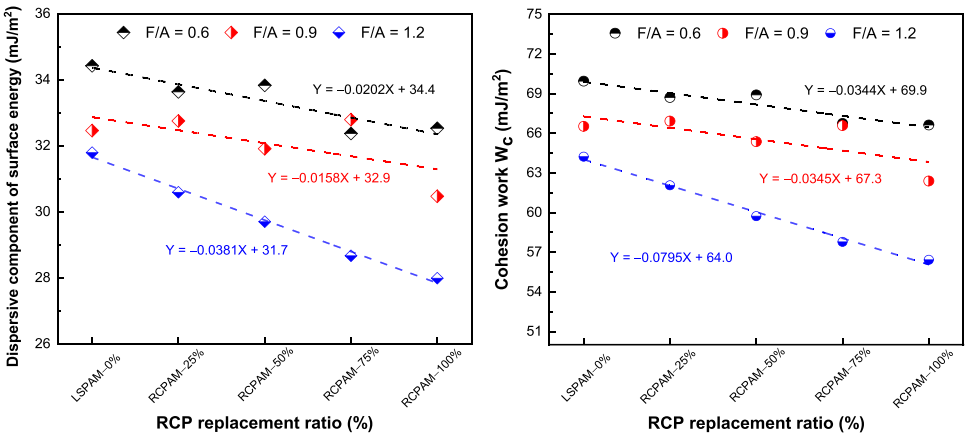

(a) Dispersive component (b) Cohesion work

Fig. 16. Variations of Dispersive component and cohesion work in terms of RCP replacement ratio for asphalt mastic with different F/A ratio.

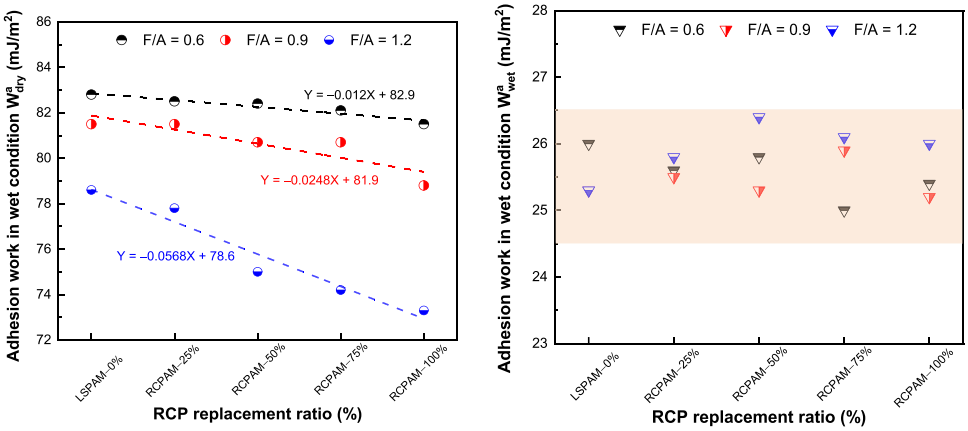

(a) Dry condition (b) Wet condition

Fig. 17. Adhesion works of MRA-RCPAM interface.

(1) Boiling water test, even with the assistance of image processing analysis, cannot properly evaluate the moisture susceptibility and adhesive characteristics between RA and RCPAM. The data variation is very large and variations regularity are unclear, possibly due to the fact the relatively small number of samples tested, and the surface properties of RA vary largely. Enlarged sample size is recommended for future research.

(2) The BBS test on modelled RA shows cohesive failure is the most common failure form for RCPAM without presence of moisture. Differently, adhesive failure dominates the failure type in the presence of moisture. The increase of both F/A and RCP replacement ratios unfavorably decrease the interfacial bond strength between RA and RCPAM.

(3) A series of multivariate linear, nonlinear, and mixed models are proposed to the predict the interfacial bond strength of RCPAM and RA at a given range of RCP replacement ratio (0–100 %), surface roughness (0–0.15) and F/A ratio (0.3–1.2). The best-fit model possesses a R^2 of 0.960 and D-W value of 1.919. Surface roughness possesses a significantly positive influence whereas RCP replacement ratio and F/A ratio possess a significantly negative influence on the bond strength of RA-RCP interface under the wet condition ($POTS_{wet}$).

(4) The SFE method reveals that the dispersive component of surface energy ($\gamma_{asphalt}$), cohesion work (W_c), and adhesion work in dry condition (W^a_{dry}) unfavorably decrease with the increase of F/A ratio and RCP replacement ratio. RCP content has less effect on the $\gamma_{asphalt}$, W_c, and W^a_{dry} of asphalt mastic when F/A ratios are 0.6 and 0.9, whereas RCP content shows more significant effect F/A is 1.2.

(5) The inclusion of RCP decreases the W_c, and W^a_{dry} but limitedly varies the W^a_{wet}. The degradations of both cohesion and adhesion under dry condition with increasing RCP content imply that the moisture damage of RCPAM is stemmed from its both cohesive

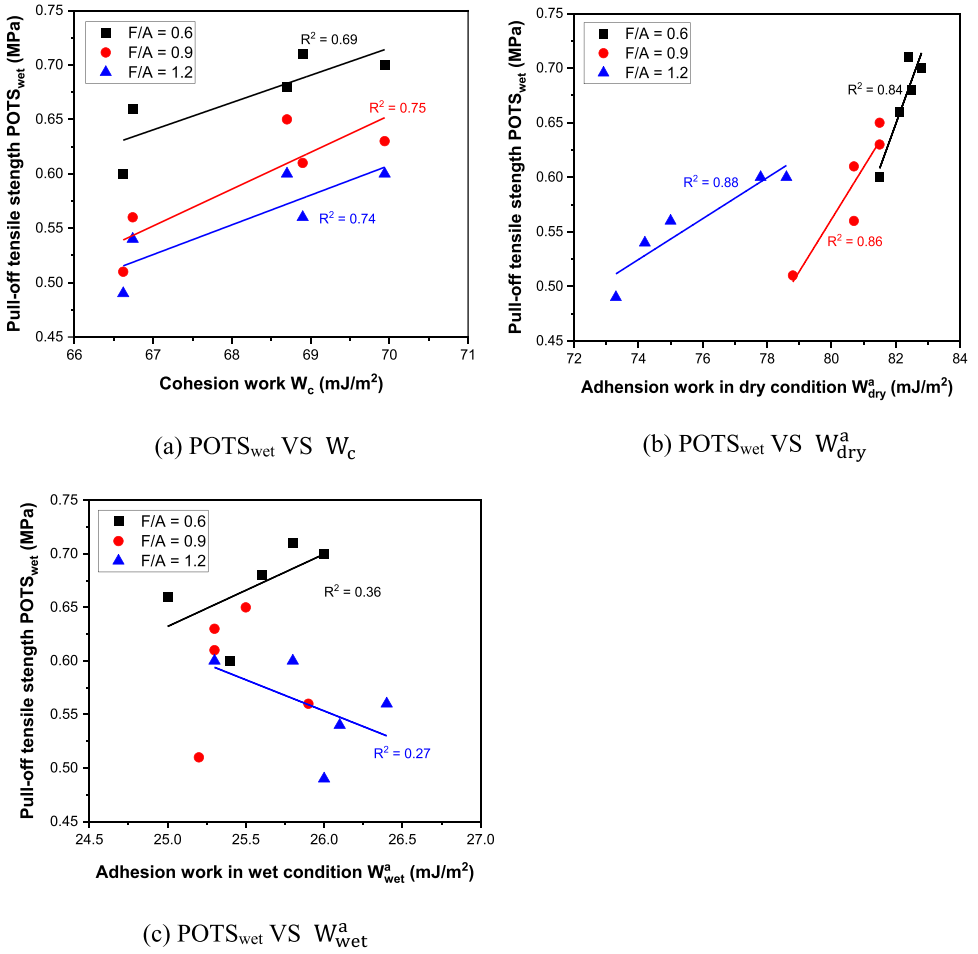

Fig. 18. Comparisons between wet pull-off strength and (a) Cohesion work, (b) Adhesion work in dry condition, and (c) Adhesion work in wet condition.

and adhesive failure, while the imperceptible impact of W^a_{wet} with increasing RCP content suggest that adhesion failure energy is limitedly impacted by the inclusion of RCP with the presence of moisture.

(6) The correlation between BBS and SFE results implies that there is not significant correlation between W^a_{wet} and bond strength for RCPAM-RA system, which shows a good agreement with the fact that the adhesion failure energy of RCPAM-RA system is limitedly impacted by the inclusion of RCP with the presence of moisture.

Overall, this study primarily evaluated macroscopic interfacial adhesion characteristics between RA and RCPAM in asphalt mixtures. RA and RCP hold significant potential as environmentally sustainable raw materials for asphalt mixtures. The results reveal that RA and RCP are feasible to substitute traditional raw materials into paving asphalt with acceptable performances in bond strength and water stability, which is in line with the sustainable development and circular economy. Future efforts should be placed on microscopic structure and chemical constituents of the adhesion interface, pavement performance, optimization of the manufacture and application processes of the sustainable asphalt mixture filled with RA and RCP. Moreover, its environmental and cost life cycle assessment are worthy conducted.

Declaration of Competing Interest

The authors declare that they have no known competing financial interests or personal relationships that could have appeared to influence the work reported in this paper.

Data availability

Data will be made available on request.

Acknowledgments

The authors would like to acknowledge the supports from National Natural Science Foundation of China (52268043, 51968046), Training Plan for Academic and Technical Leaders of Major Disciplines in Jiangxi Province-Leading Talent Project (20204BCJ22003), Australian Research Council (ARC), Australia, and University of Technology Sydney Research Academic Program at Tech Lab (UTS RAPT). The third and fourth authors also appreciate the China Scholarship Council (CSC).

References

[1] R. Xiao, P. Polaczyk, B. Huang, Measuring moisture damage of asphalt mixtures: the development of a new modified boiling test based on color image processing, Measurement 190 (2022), 110699.
[2] R. Xiao, P. Polaczyk, Y. Wang, Y. Ma, H. Lu, B. Huang, Measuring moisture damage of hot-mix asphalt (HMA) by digital imaging-assisted modified boiling test (ASTM D3625): recent advancements and further investigation, Constr. Build. Mater. 350 (2022), 128855.
[3] Y. Ma, P. Polaczyk, R. Xiao, X. Jiang, M. Zhang, Y. Liu, B. Huang, Influence of mobilized RAP content on the effective binder quality and performance of 100% hot in-place recycled asphalt mixtures, Constr. Build. Mater. 342 (2022), 127941.
[4] S. Caro, E. Masad, A. Bhasin, D.N. Little, Moisture susceptibility of asphalt mixtures, Part 1: mechanisms, Int. J. Pavement Eng. 9 (2) (2008) 81–98.
[5] F. Guo, J. Pei, J. Zhang, B. Xue, G. Sun, R. Li, Study on the adhesion property between asphalt binder and aggregate: a state-of-the-art review, Constr. Build. Mater. 256 (2020), 119474.
[6] J.P. Aguiar-Moya, A. Baldi-Sevilla, J. Salazar-Delgado, J.F. Pacheco-Fallas, L. Loria-Salazar, F. Reyes-Lizcano, N. Cely-Leal, Adhesive properties of asphalts and aggregates in tropical climates, Int. J. Pavement Eng. 19 (8) (2018) 738–747.
[7] B. Lei, W. Li, Z. Tang, V.W. Tam, Z. Sun, Durability of recycled aggregate concrete under coupling mechanical loading and freeze-thaw cycle in salt-solution, Constr. Build. Mater. 163 (2018) 840–849.
[8] C. Shi, Y. Li, J. Zhang, W. Li, L. Chong, Z. Xie, Performance enhancement of recycled concrete aggregate–a review, J. Clean. Prod. 112 (2016) 466–472.
[9] J. Xiao, W. Li, Y. Fan, X. Huang, An overview of study on recycled aggregate concrete in China (1996–2011), Constr. Build. Mater. 31 (2012) 364–383.
[10] Q. Liu, B. Li, J. Xiao, A. Singh, Utilization potential of aerated concrete block powder and clay brick powder from C&D waste, Constr. Build. Mater. 238 (2020), 117721.
[11] Z. Duan, S. Hou, J. Xiao, B. Li, Study on the essential properties of recycled powders from construction and demolition waste, J. Clean. Prod. 253 (2020), 119865.
[12] S. Li, J. Gao, Q. Li, X. Zhao, Investigation of using recycled powder from the preparation of recycled aggregate as a supplementary cementitious material, Constr. Build. Mater. 267 (2021), 120976.
[13] S. Li, Q. Li, X. Zhao, J. Luo, S. Gao, G. Yue, D. Su, Experimental study on the preparation of recycled admixtures by using construction and demolition waste, Materials 12 (10) (2019) 1678.
[14] J. Xiao, Z. Ma, T. Sui, A. Akbarnezhad, Z. Duan, Mechanical properties of concrete mixed with recycled powder produced from construction and demolition waste, J. Clean. Prod. 188 (2018) 720–731.
[15] Q. Liu, T. Tong, S. Liu, D. Yang, Q. Yu, Investigation of using hybrid recycled powder from demolished concrete solids and clay bricks as a pozzolanic supplement for cement, Constr. Build. Mater. 73 (2014) 754–763.
[16] M. Chen, J. Lin, S. Wu, Potential of recycled fine aggregates powder as filler in asphalt mixture, Constr. Build. Mater. 25 (10) (2011) 3909–3914.
[17] V. Antunes, A. Freire, L. Quaresma, R. Micaelo, Evaluation of waste materials as alternative sources of filler in asphalt mixtures, Mater. Struct. 50 (2017) 1–13.
[18] D.-W. Cho, H.U. Bahia, Effects of aggregate surface and water on rheology of asphalt films, Transp. Res. Rec. 1998 (1) (2007) 10–17.
[19] F. Canestrari, F. Cardone, A. Graziani, F.A. Santagata, H.U. Bahia, Adhesive and cohesive properties of asphalt-aggregate systems subjected to moisture damage, Road. Mater. Pavement Des. 11 (sup1) (2010) 11–32.
[20] Q. Huang, Z. Qian, J. Hu, D. Zheng, L. Chen, M. Zhang, J. Yu, Investigation on the properties of aggregate-mastic interfacial transition zones (ITZs) in asphalt mixture containing recycled concrete aggregate, Constr. Build. Mater. 269 (2021), 121257.
[21] X. Ji, E. Sun, H. Zou, Y. Hou, B. Chen, Study on the multiscale adhesive properties between asphalt and aggregate, Constr. Build. Mater. 249 (2020), 118693.
[22] X. Ji, Y. Hou, H. Zou, B. Chen, Y. Jiang, Study of surface microscopic properties of asphalt based on atomic force microscopy, Constr. Build. Mater. 242 (2020), 118025.
[23] Y. Hou, X. Ji, J. Li, X. Li, Adhesion between asphalt and recycled concrete aggregate and its impact on the properties of asphalt mixture, Materials 11 (12) (2018) 2528.
[24] Q. Tang, P. Xiao, C. Kou, K. Lou, A. Kang, Z. Wu, Physical, chemical and interfacial properties of modified recycled concrete aggregates for asphalt mixtures: a review, Constr. Build. Mater. 312 (2021), 125357.
[25] L. Wang, A. Shen, J. Yao, Effect of different coarse aggregate surface morphologies on cement emulsified asphalt adhesion, Constr. Build. Mater. 262 (2020), 120030.
[26] A. Pasandín, I. Pérez, Effect of ageing time on properties of hot-mix asphalt containing recycled concrete aggregates, Constr. Build. Mater. 52 (2014) 284–293.
[27] B. Lei, Q. Xiong, Z. Tang, Z. Yao, J. Jiang, Effect of recycled aggregate modification on the properties of permeable asphalt concrete, Sustainability 14 (17) (2022) 10495.
[28] Z. Zhang, K. Wang, H. Liu, Z. Deng, Key performance properties of asphalt mixtures with recycled concrete aggregate from low strength concrete, Constr. Build. Mater. 126 (2016) 711–719.
[29] L. Ding, J. Zhang, B. Feng, C. Li, Performance evaluation of recycled asphalt mixtures containing construction and demolition waste applicated as pavement base, Adv. Civ. Eng. 2020 (2020) 1–11.
[30] H.K.A. Al-Bayati, S.L. Tighe, J. Achebe, Influence of recycled concrete aggregate on volumetric properties of hot mix asphalt, Resour. Conserv. Recycl. 130 (2018) 200–214.
[31] A.I. Kareem, H. Nikraz, H. Asadi, Evaluation of the double coated recycled concrete aggregates for hot mix asphalt, Constr. Build. Mater. 172 (2018) 544–552.
[32] M.S. Pourtahmasb, M.R. Karim, Performance evaluation of stone mastic asphalt and hot mix asphalt mixtures containing recycled concrete aggregate, Adv. Mater. Sci. Eng. 2014 (2014).
[33] B. Lei, Q. Xiong, H. Zhao, W. Dong, V.W. Tam, Z. Sun, W. Li, Performance of asphalt mortar with recycled concrete powder under different filler-to-asphalt weight ratios, Case Stud. Constr. Mater. (2023), e01834.
[34] Q. Liu, S. Cheng, C. Sun, K. Chen, W. Li, V.W.Y. Tam, Steel cable bonding in fresh mortar and 3D printed beam flexural behavior, Autom. Constr. 158 (2024) 105165.
[35] P. Zhan, J. Wang, H. Zhao, W. Li, S.P. Shah, J. Xu, Impact of synthetic C-S-H seeds on early hydration and pore structure evolution of cement pastes: A study by ^{1}H low-field NMR and path analysis, Cem. Concr. Res. 175 (2024) 107376.
[36] X. Lin, W. Li, A. Castel, T. Kim, Y. Huang, A comprehensive review on self-healing cementitious composites with crystalline admixtures: Design, performance and application, Constr. Build. Mater. 409 (2023) 134108.
[37] R. Mi, Y. Wang, T. Yu, W. Li, Effects of carbon-sequestering coral aggregate on pore structures and compressive strength of concrete, Low-carbon Materials and Green, Construction 1 (1) (2023) 21.
[38] i.C. Common Portland cement (GB/T 175–2007). Standards Press of China.
[39] China, J.T.G. F40–2017. Technical Specifications for Construction of Highway Asphalt Pavement, 2017.
[40] P.M.D. Santos, E.N.B.S. Júlio, Comparison of methods for texture assessment of concrete surfaces, Acids Mater. J. 107 (5) (2010).

[41] Mo.TotPs.Ro China, Standard Test Methods of Bitumen and Bituminous Mixtures for Highway Engineering (JTGE20-2011/T 0616-1993), China Communications Press, Beijing, 2011, 2011.
[42] J.P. Aguiar-Moya, J. Salazar-Delgado, A. Baldi-Sevilla, F. Leiva-Villacorta, L. Loria-Salazar, Effect of aging on adhesion properties of asphalt mixtures with the use of bitumen bond strength and surface energy measurement tests, Transp. Res. Rec. 2505 (1) (2015) 57–65.
[43] L. Zhou, W. Huang, Y. Zhang, Q. Lv, C. Yan, Y. Jiao, Evaluation of the adhesion and healing properties of modified asphalt binders, Constr. Build. Mater. 251 (2020), 119026.
[44] S. Liu, S. Zhou, A. Peng, Analysis of moisture susceptibility of foamed warm mix asphalt based on cohesion, adhesion, bond strength, and morphology, J. Clean. Prod. 277 (2020), 123334.
[45] P. Li, G. Fu, D. Yang, G. Hu, J. Zheng, Research on effects of deicing salt on adhesion properties between asphalt mortar and aggregate, Prz. Elektrotech. 88 (1B) (2012) 127–131.
[46] Y. Han, B. Cui, J. Tian, J. Ding, F. Ni, D. Lu, Evaluating the effects of styrene-butadiene rubber (SBR) and polyphosphoric acid (PPA) on asphalt adhesion performance, Constr. Build. Mater. 321 (2022), 126028.
[47] P. Cui, S. Wu, Y. Xiao, F. Wang, F. Wang, Quantitative evaluation of active based adhesion in Aggregate-Asphalt by digital image analysis, J. Adhes. Sci. Technol. 33 (14) (2019) 1544–1557.
[48] M. Nazirizad, A. Kavussi, A. Abdi, Evaluation of the effects of anti-stripping agents on the performance of asphalt mixtures, Constr. Build. Mater. 84 (2015) 348–353.
[49] R. Xiao, J. Guo, Y. Ding, P. Polaczyk, Y. Ma, X. Jiang, B. Huang, Evaluating asphalt mix ingredients by moisture susceptibility: the development of a new modified boiling test procedure based on digital imaging, J. Mater. Civ. Eng. 34 (11) (2022) 04022293.
[50] Q. Chen, C. Wang, Z. Qiao, T. Guo, Graphene/tourmaline composites as a filler of hot mix asphalt mixture: preparation and properties, Constr. Build. Mater. 239 (2020), 117859.
[51] C. Wang, Q. Chen, T. Guo, Q. Li, Environmental effects and enhancement mechanism of graphene/tourmaline composites, J. Clean. Prod. 262 (2020), 121313.
[52] Y. Hou, J. Li, X. Ji, H. Zou, C. Wang, X. Fang, Moisture damage of asphalt based on adhesion, microsurface energy, and nanosurface roughness, J. Mater. Civ. Eng. 34 (10) (2022) 04022249.
[53] M. Xu, J. Yi, D. Feng, Y. Huang, D. Wang, Analysis of adhesive characteristics of asphalt based on atomic force microscopy and molecular dynamics simulation, ACS Appl. Mater. Interfaces 8 (19) (2016) 12393–12403.
[54] K. Kanitpong, H. Bahia, Relating adhesion and cohesion of asphalts to the effect of moisture on laboratory performance of asphalt mixtures, Transp. Res. Rec. 1901 (1) (2005) 33–43.
[55] Q. Lv, W. Huang, N. Tang, F. Xiao, Comparison and relationship between indices for the characterization of the moisture resistance of asphalt–aggregate systems, Constr. Build. Mater. 168 (2018) 580–589.
[56] R. Shao, C. Wu, J. Li, Z. Liu, Investigation on the mechanical characteristics of multiscale mono/hybrid steel fibre-reinforced dry UHPC, Cem. Concr. Compos. 133 (2022), 104681.
[57] R. Jin, Q. Chen, A.B. Soboyejo, Non-linear and mixed regression models in predicting sustainable concrete strength, Constr. Build. Mater. 170 (2018) 142–152.
[58] R. Jin, L. Yan, A.B. Soboyejo, L. Huang, B. Kasal, Multivariate regression models in estimating the behavior of FRP tube encased recycled aggregate concrete, Constr. Build. Mater. 191 (2018) 216–227.
[59] Y. Tan, M. Guo, Using surface free energy method to study the cohesion and adhesion of asphalt mastic, Constr. Build. Mater. 47 (2013) 254–260.
[60] J. Jin, Y. Tan, R. Liu, J. Zheng, J. Zhang, Synergy effect of attapulgite, rubber, and diatomite on organic montmorillonite-modified asphalt, J. Mater. Civ. Eng. 31 (2) (2019) 04018388.
[61] Z. Sun, S. Li, J. Zhang, Y. Zeng, Adhesion property of bituminous crack sealants to different asphalt mixtures based on surface energy theory, Constr. Build. Mater. 261 (2020), 120006.
[62] K. Christmann, Introduction to surface physical chemistry, Springer Science & Business Media, 2013.